Zeeman Effect

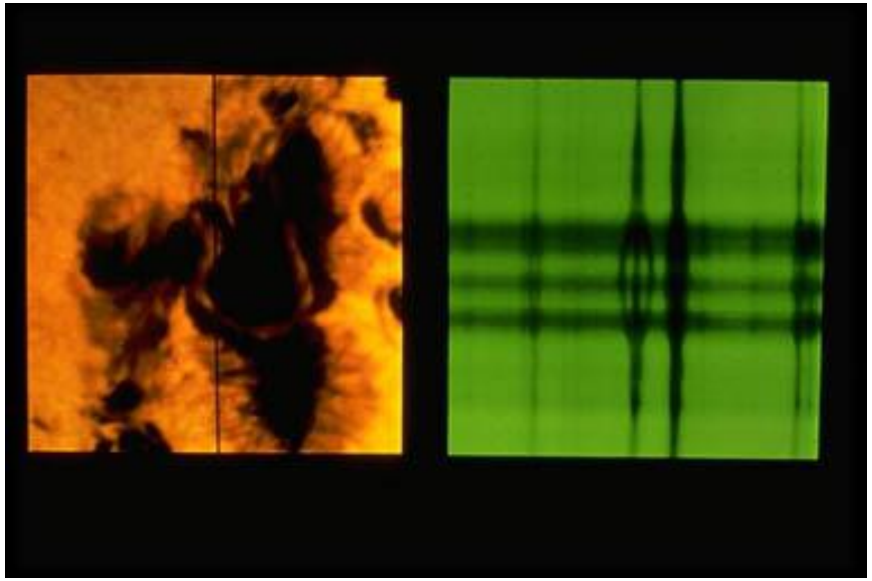

… the split of a spectral line into several components in the presence of a **magnetic field**. It is analogous to the **Stark effect**, the splitting of a spectral line into several components in the presence of an **electric field**.

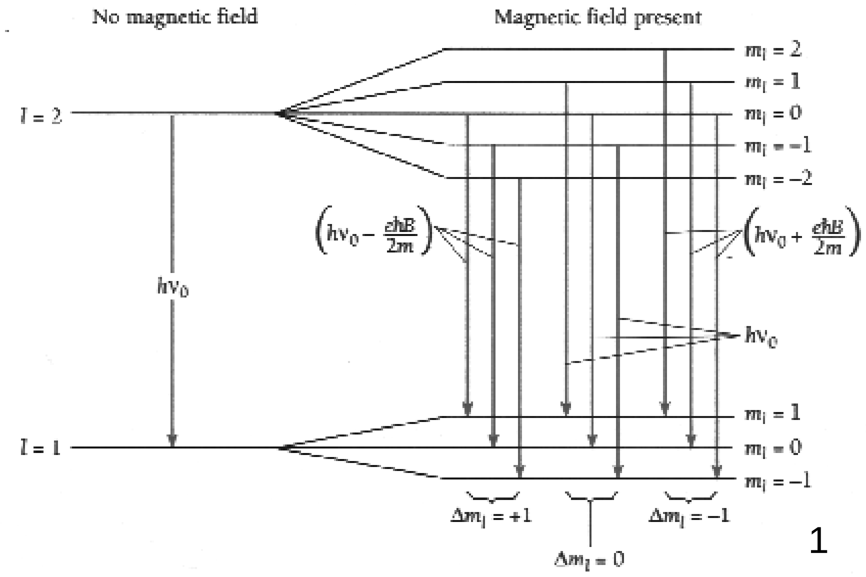

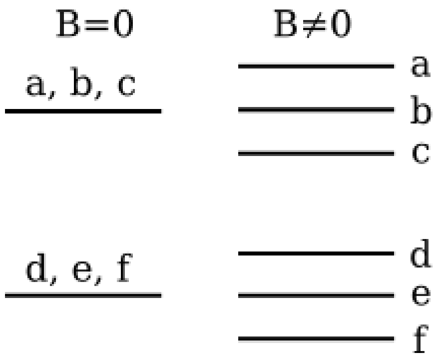

Selection Rule:

$\Delta m_F = 0, \pm 1$, but a level with $m_F = 0$ cannot combine with another $m_F = 0$

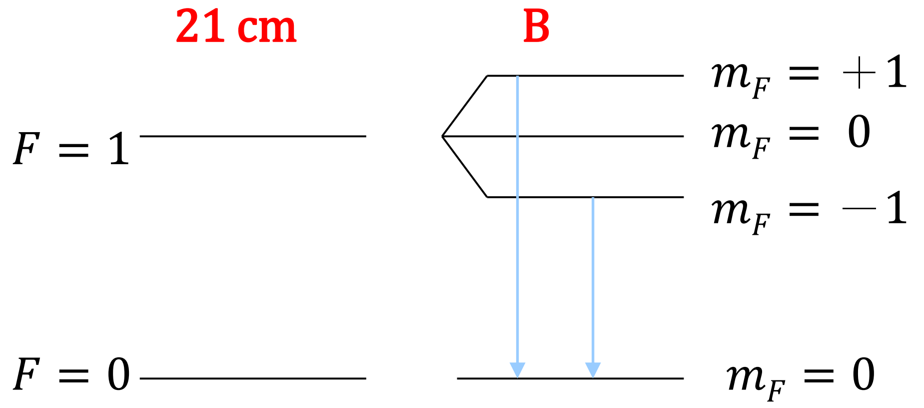

Singlet line → σ, π, σ

F: coupling of net orbital angular momentum and the net nuclear spin

$-\dfrac{eB}{4\pi m_e c}$	ν_{mn}	$+\dfrac{eB}{4\pi m_e c}$
Elliptical polarization	Plane polarization	Elliptical polarization

$$\frac{eB}{4\pi m_e c} = 1.4 \times 10^6 \; B_{\text{Gauss}} \; [\text{Hz}]$$ **Larmor frequency of precession**

Along $\vec{B}$, $\pi = 0$, σs are circularly polarized in opposite directions

Total splitting $\Delta\nu = 2.80 \times 10^6 \ B_{\rm Gauss}$ [Hz]

Typically in ISM, $B \sim 10^{-6}$ Gauss, so $\Delta\nu \sim$ a few hertzs $\quad < B_{\rm Galactic} > \sim 4 \ \mu$G

very difficult to detect ($\ll$ Doppler width)

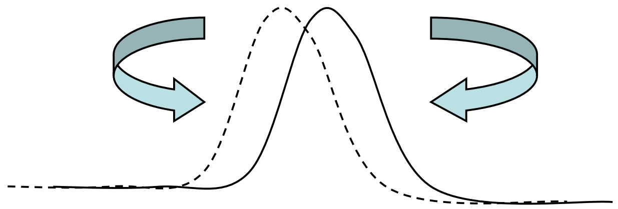

Zeeman splitting was first detected in 21-cm absorption (Verschuur 1969); later seen in emission, too (Heiles 1982)

… also has been observed in OH 18 cm and 6 cm H_2CO 6 cm lines

➔ to derive B and n (HI)

$B \propto n^{\alpha}$ for H I clouds, $\alpha \sim 2/3$ to $1/3$

(the denser the cloud, the stronger the magnetic field)

Note: For an isotropically contracting cloud with a "frozen-in" magnetic field, $B \propto 1/R^2$, and because $\rho \propto 1/R^3 \Rightarrow \boxed{B \propto n_H^{2/3}}$

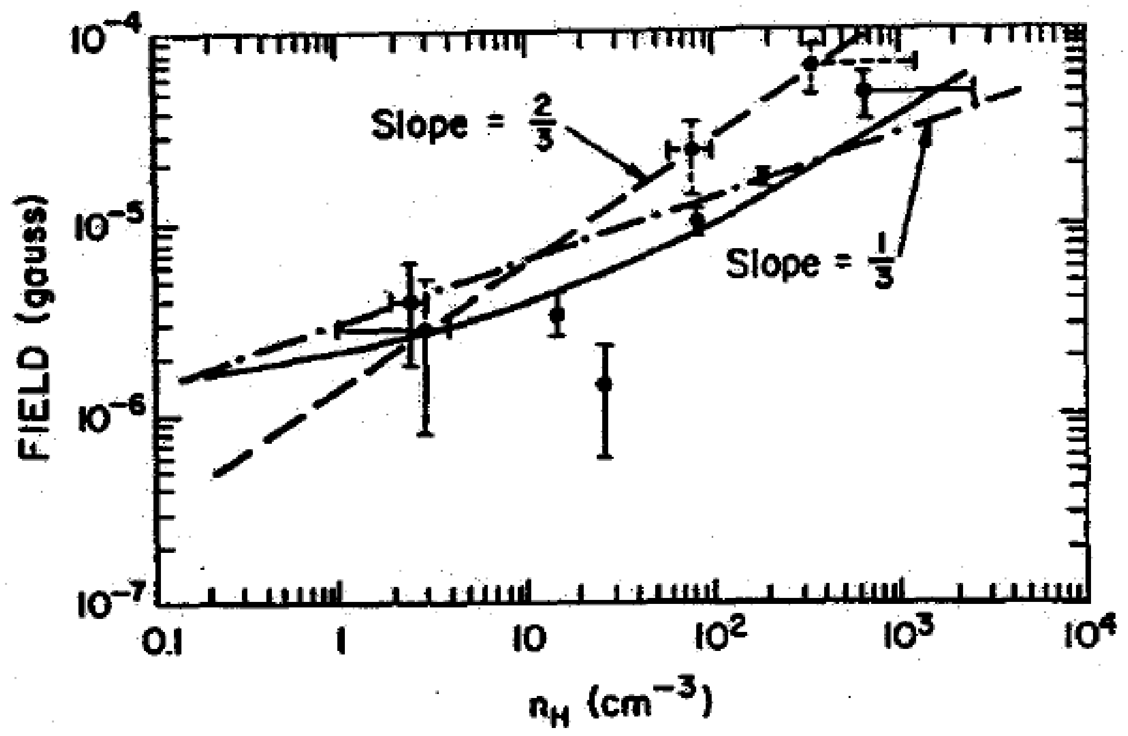

Fig. 1. Magnetic field strength in H I clouds as a function of gas density.

Magnetic field does not intensify as the density increases, as the frozen-in assumption predicts
--- there is "flux leakage"

Mouschovias (1983) Adv. Space Res. 2, 71

THE ASTROPHYSICAL JOURNAL, **301**:339–345, 1986 February 1

INTERSTELLAR MAGNETIC FIELD STRENGTHS AND GAS DENSITIES: OBSERVATIONAL AND THEORETICAL PERSPECTIVES

T. H. TROLAND
Physics and Astronomy Department, University of Kentucky

AND

CARL HEILES
Astronomy Department, University of California, Berkeley

Received 1985 January 31, accepted 1985 July 16

ABSTRACT

We present an updated compilation of observational data concerning the relationship between the interstellar magnetic field strength and the gas density. Pulsar and Zeeman-effect data provide the only reliable information about the (B, n) relationship, and they now span nearly six orders of magnitude in gas density. Field strengths show no evidence of increase over the density range $0.1\text{–}{\sim}100\ \text{cm}^{-3}$. At higher densities, a modest increase in field strength is observed in some regions, in line with theoretical expectations for self-gravitating clouds. In two regions of the interstellar medium, the magnetic field is unusually high; however, these are not locales where self-gravitation is important. Despite the consistency between observations and theory, questions still exist about how the magnetic field strength remains constant for densities up to ${\sim}100\ \text{cm}^{-3}$. Further Zeeman effect studies and a better theoretical understanding of the formation of interstellar clouds and complexes will be necessary to answer these questions.

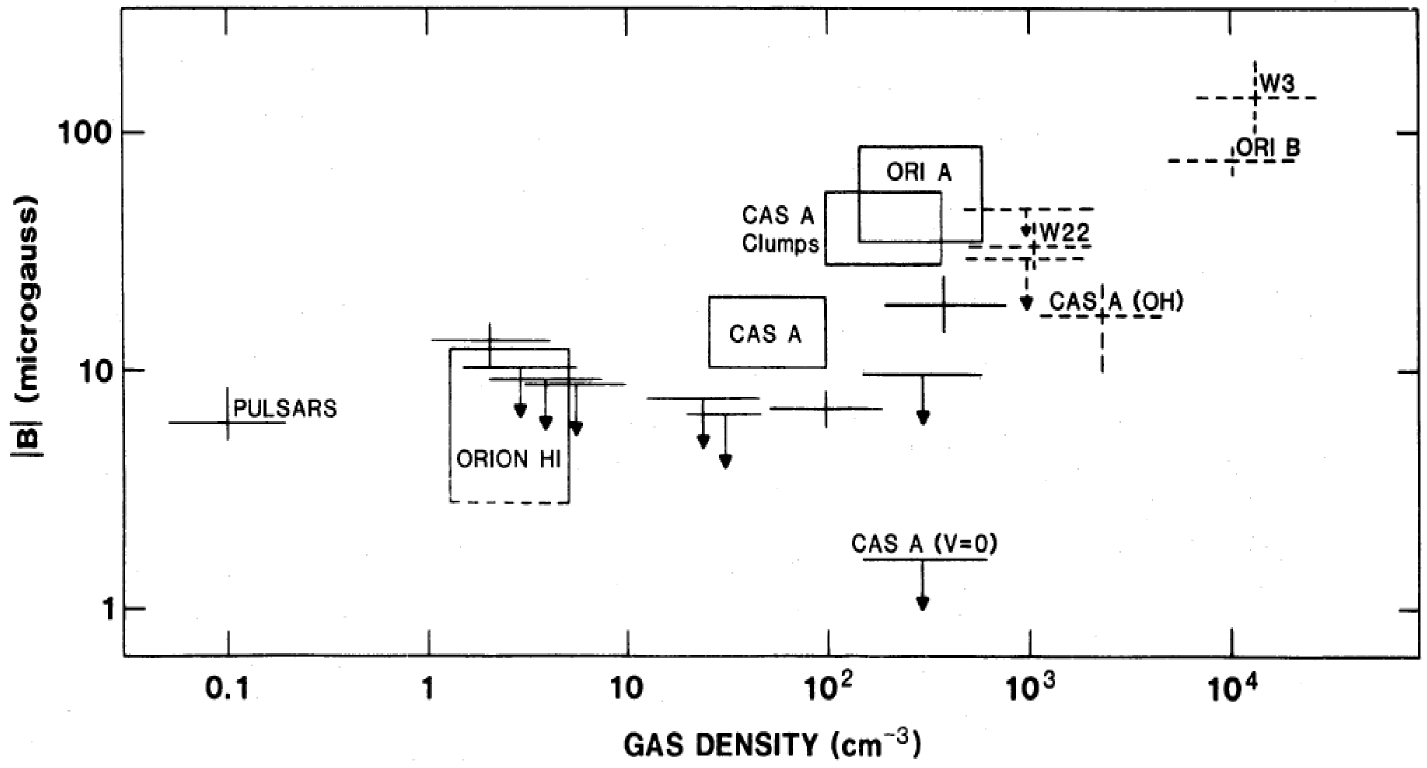

FIG. 1.—Observed magnetic field strengths as a function of estimated volume density. All results come from measurements of the H I (*solid lines*) and OH (*dashed lines*) Zeeman effect, except for the point labeled "pulsars." This point is derived from pulsar rotation and dispersion measures. Rectangular boxes represent ranges of field strengths encountered in Zeeman effect maps made either with a single-dish or with aperture synthesis instruments. See § II for further details.

Troland & Heiles (1986) ApJ, 301, 339

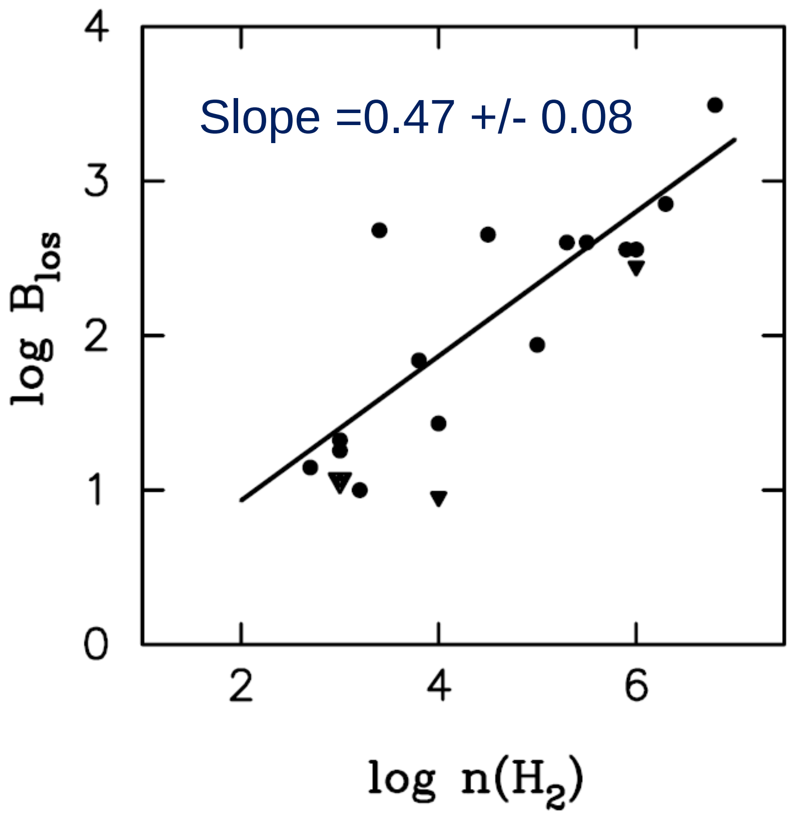

FIG. 1.—Plot of log B_{los} vs. log $n(H_2)$. Inverted triangles are the upper limits for undetected clouds; the averaged limit for all of the dark clouds with log $n(H_2) = 3$ is plotted as a single large inverted triangle. The line is the fit to detected clouds.

MAGNETIC FIELDS IN MOLECULAR CLOUDS: OBSERVATIONS CONFRONT THEORY

RICHARD M. CRUTCHER
Astronomy Department, University of Illinois, Urbana, IL 61801
Received 1998 November 16; accepted 1999 March 5

ABSTRACT

This paper presents a summary of all 27 available sensitive Zeeman measurements of magnetic field strengths in molecular clouds together with other relevant physical parameters. From these data input parameters to magnetic star formation theory are calculated, and predictions of theory are compared with observations. Results for this cloud sample are the following: (1) Internal motions are supersonic but approximately equal to the Alfvén speed, which suggests that supersonic motions are likely MHD waves. (2) The ratio of thermal to magnetic pressures $\beta_p \approx 0.04$, implying that magnetic fields are important in the physics of molecular clouds. (3) The mass–to–magnetic flux ratio is about twice critical, which suggests but does not require that static magnetic fields alone are insufficient to support clouds against gravity. (4) Kinetic and magnetic energies are approximately equal, which suggests that static magnetic fields and MHD waves are roughly equally important in cloud energetics. (5) Magnetic field strengths scale with gas densities as $|\boldsymbol{B}| \propto \rho^{\kappa}$ with $\kappa \approx 0.47$; this agrees with the prediction of ambipolar diffusion driven star formation, but this scaling may also be predicted simply by Alfvénic motions. The measurements of magnetic field strengths in molecular clouds make it clear that magnetic fields are a crucial component of the physics governing cloud evolution and star formation.

Crutcher 1999, ApJ, 520, 706

Magnetic field strengths in galaxies determined by intensity of synchrotron emission, assuming equi-partion between magnetic field and cosmic rays.

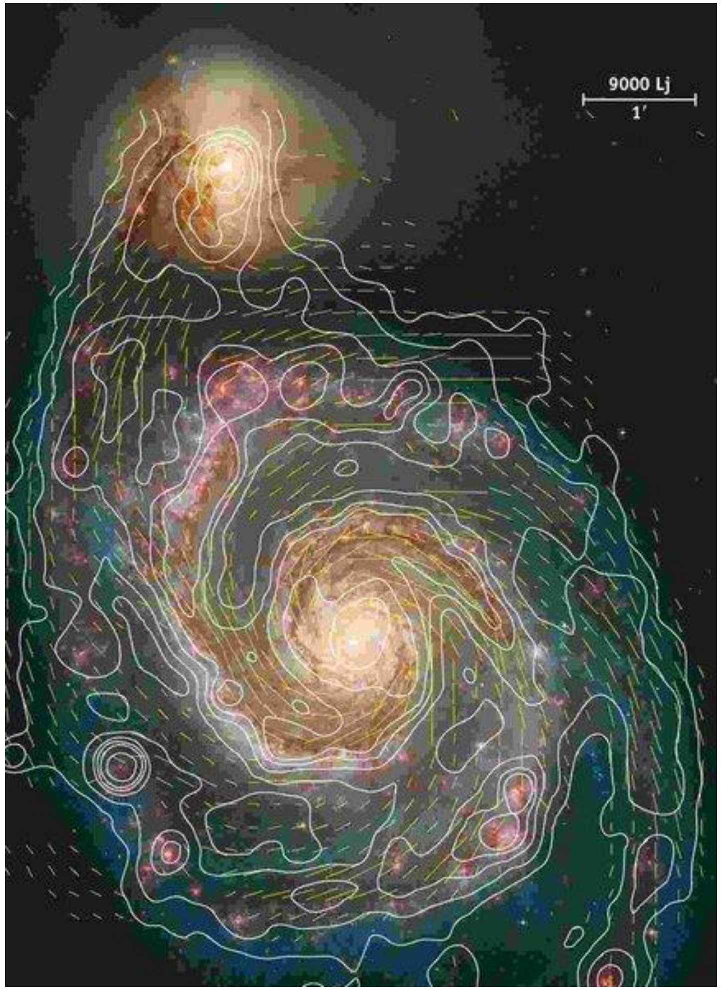

Figure 1: Optical image of the spiral galaxy M 51 obtained with the Hubble Space Telescope (from Hubble Heritage), overlaid by contours of the total radio intensity and polarization vectors at 6cm wavelength, combined from radio observations with the Effelsberg and VLA radio telescopes (from Fletcher and Beck, in prep.). The magnetic field follows well the optical spiral structure, but the regions between the spiral arms also contain strong and ordered fields. The bar in the top right corner indicates a scale of 1 arcminute or about 9000 light years (about 3 kiloparsecs) at the distance of the galaxy. Copyright: MPIfR Bonn

http://www.scholarpedia.org/article/Galactic_magnetic_fields

Polarized Starlight

Magnetic field in the ISM first discerned by linearly polarized starlight (~1%) (Hiltner 1949 and Hall 1949)

It is thought that the partial polarization of starlight is produced by elongated dust grains aligned by magnetic fields in the ISM (see a review by Lazarian astro-ph 0003314 "*Physics of Grain Alignment*")

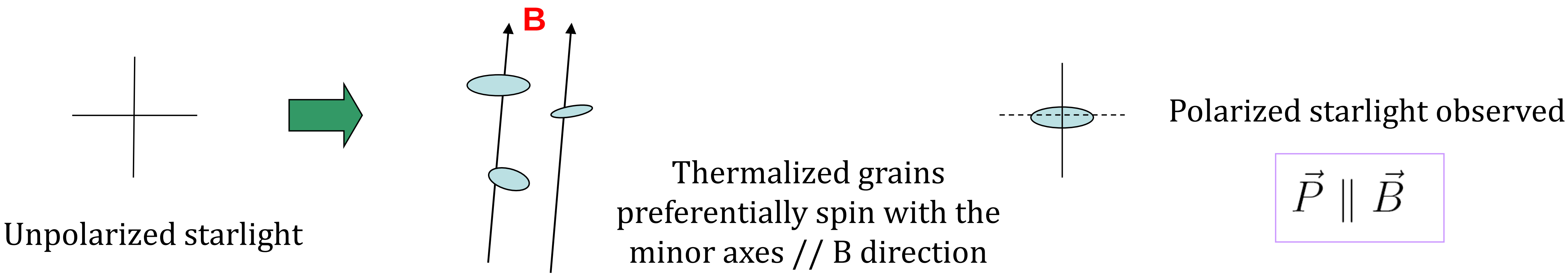

$$\vec{P} \parallel \vec{B}$$

A thermalized ISM elongated grain tends to spin along its minor axis: $\vec{\omega} \longrightarrow \vec{\mathrm{B}}$

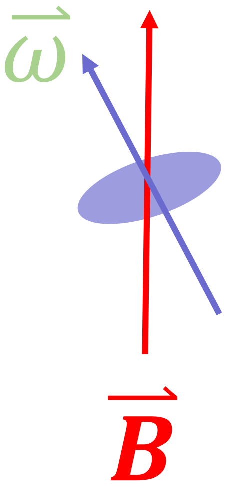

Davis-Greenstein alignment mechanism --- paramagnetic dissipation

http://bgandersson.net/grain-alignment

Observations in OIR

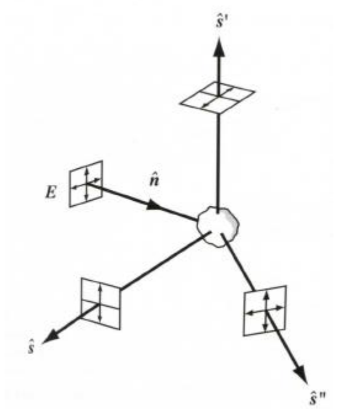

Scattering by dust

Stahler & Pallo 2004

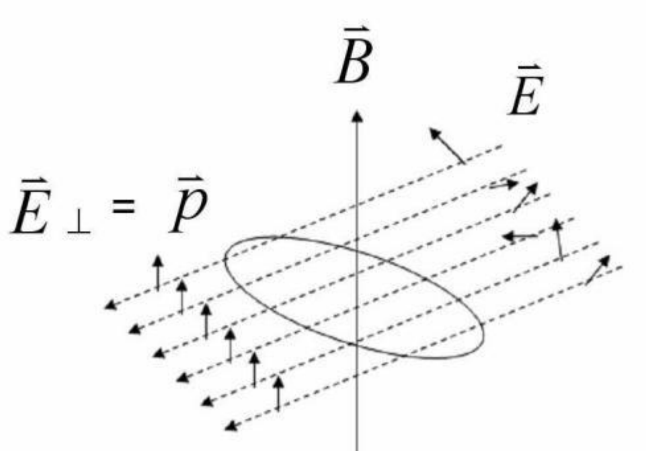

Dichroic extinction by aligned dust

Observations in FIR to mm

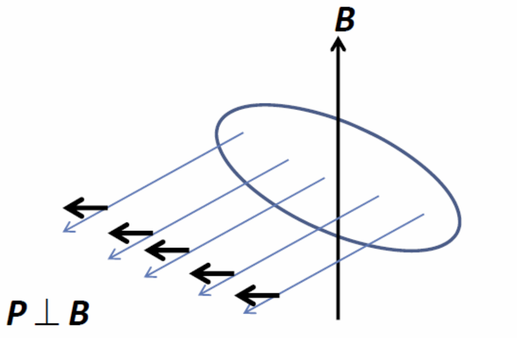

Polarized thermal emission by dust aligned by ***B***

Courtesy: Tamura

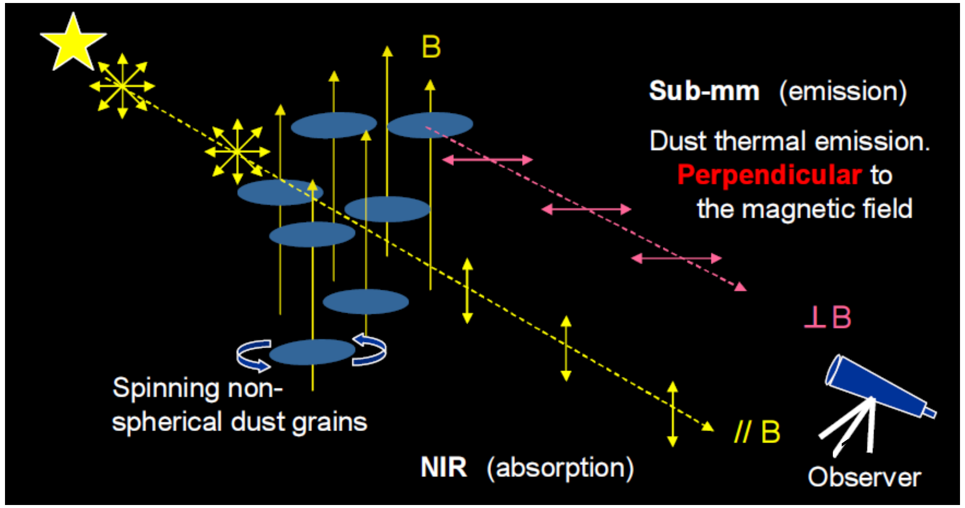

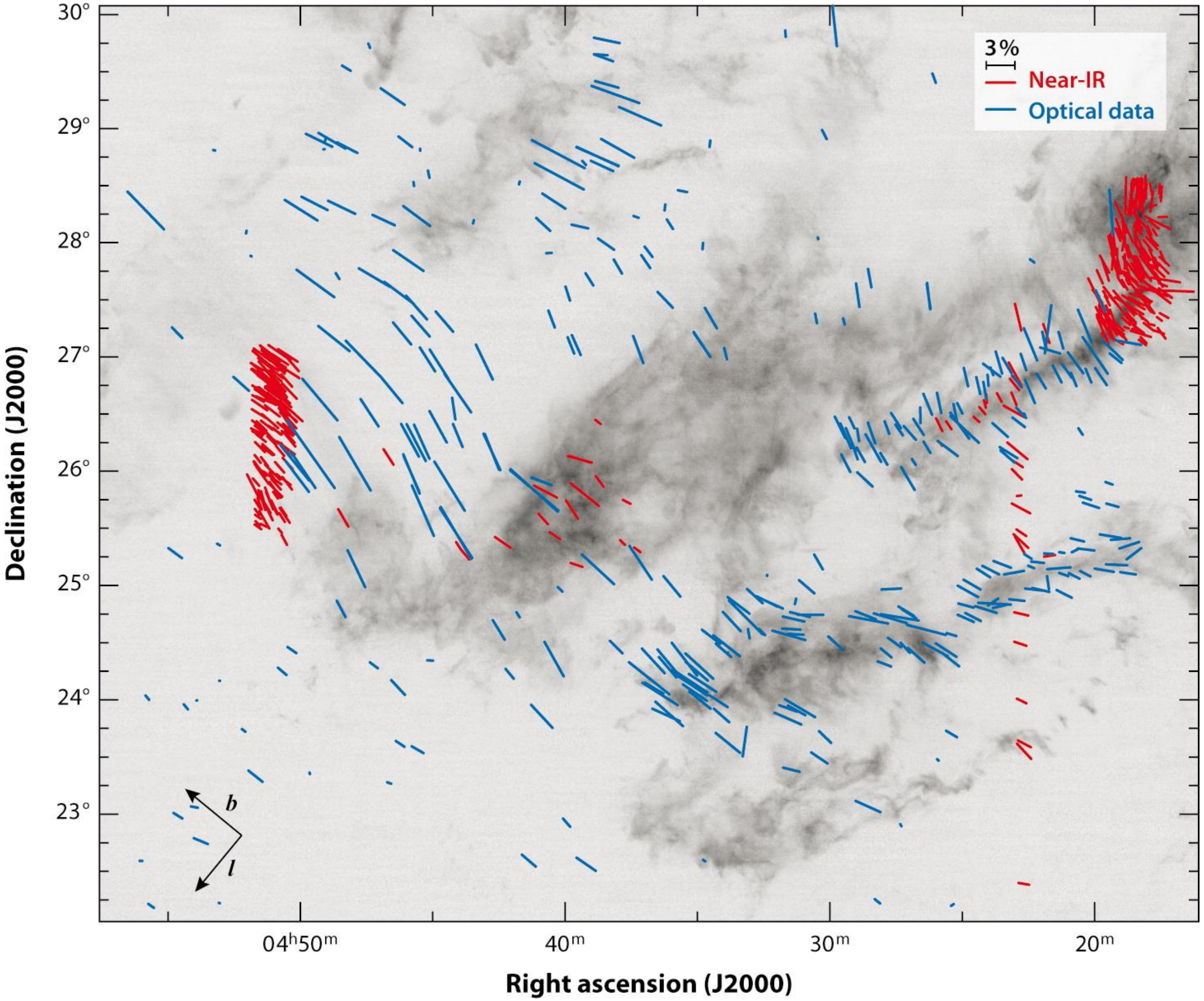

Crutcher RM. 2012.
Annu. Rev. Astron. Astrophys. 50:29–63

Organized magnetic field morphology in the Taurus dark-cloud complex superposed on a ^{13}CO map (Chapman et al. 2011). Blue lines show polarization measured at optical wavelengths and red lines show near-IR (*H*-band and *I*-band) polarization.

Dichroic extinction by dust (optical and near-IR)

$$\vec{P} \parallel \vec{B}$$

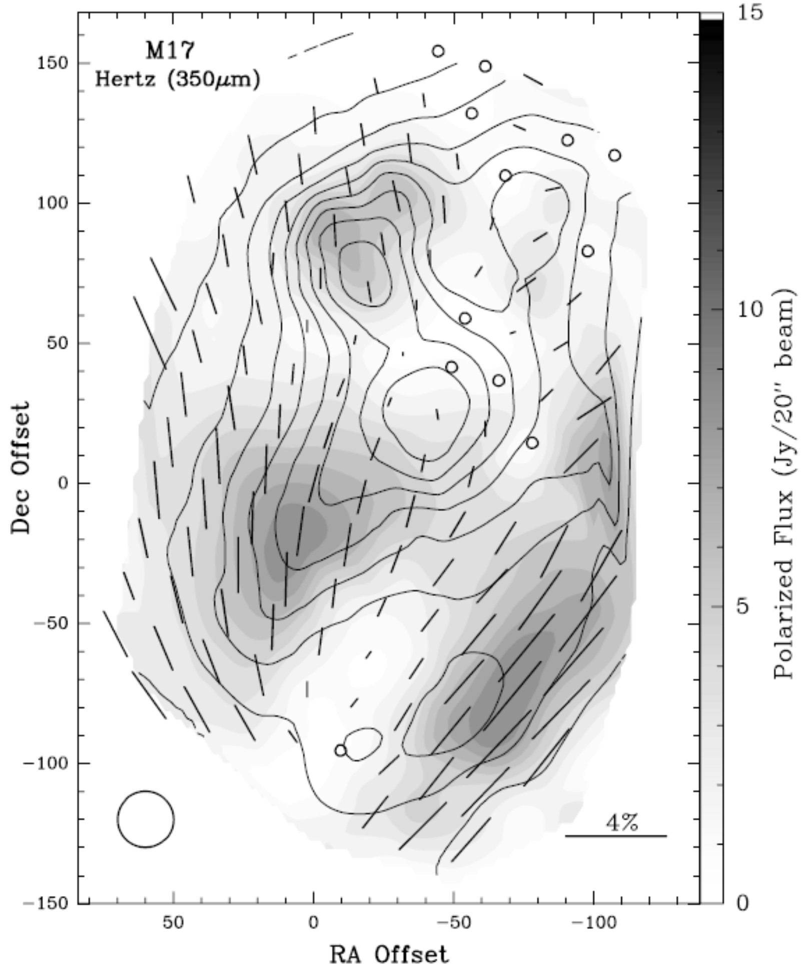

FIG. 6.—HERTZ polarization map of M17 at 350 μm. All of the polarization vectors shown have a polarization level and error such that $P > 3\sigma_P$. Circles indicate cases where $P + 2\sigma_P < 1\%$. The contours delineate the total continuum flux (from 10% to 90% with a maximum flux of ≈700 Jy), whereas the underlying gray scale gives the polarized flux according to the scale on the right. The beam width (≃20″) is shown in the lower left corner and the origin of the map is at R.A. = $18^h17^m31^s.4$, decl. = −16°14′25″.0 (B1950.0).

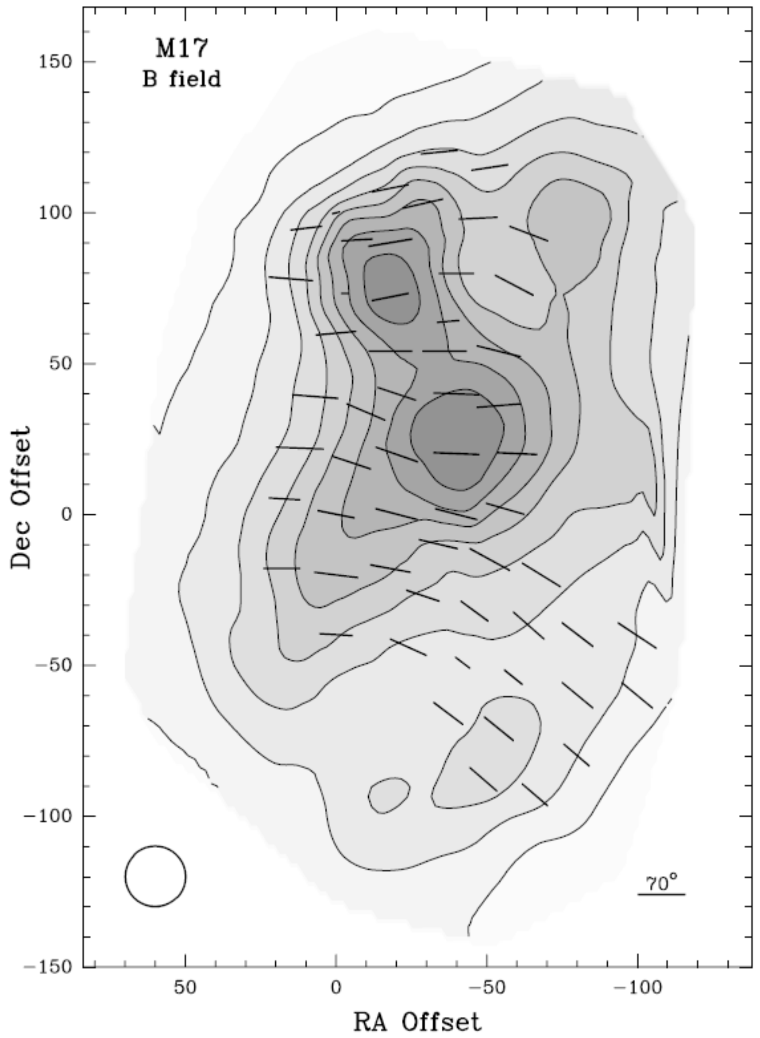

FIG. 11.—Orientation of the magnetic field in M17. The orientation of the projection of the magnetic field in the plane of the sky is shown by the vectors and the viewing angle is given by the length of the vectors (using the scale shown in the bottom right corner). The contours and the gray scale delineate the total continuum flux. The beam width (≃20″) is shown in the lower left corner, and the origin of the map is at R.A. = $18^h17^m31^s.4$, decl. = −16°14′25″.0 (B1950.0).

Thermal emission by dust (far-IR, and smm)

$\vec{P} \perp \vec{B}$

Houde et al. (2002)

Pulsar Dispersion

Shape of the same pulse varies with freq.

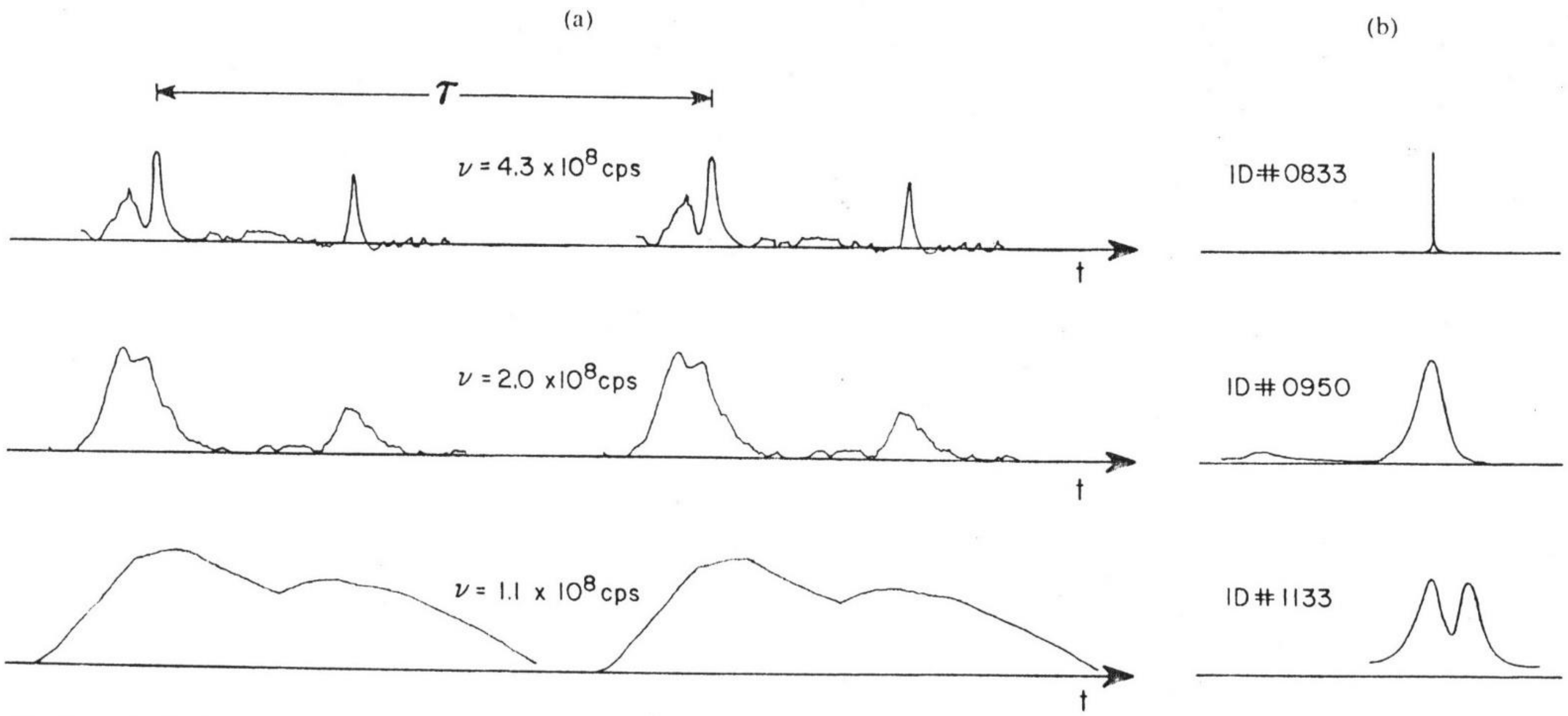

Fig. 5.8. Radio frequency detection of pulsars: (a) periodic pulse shape varying with frequency for a single pulsar; (b) integrated pulse shape for various pulsars.

Every pulsar is different.

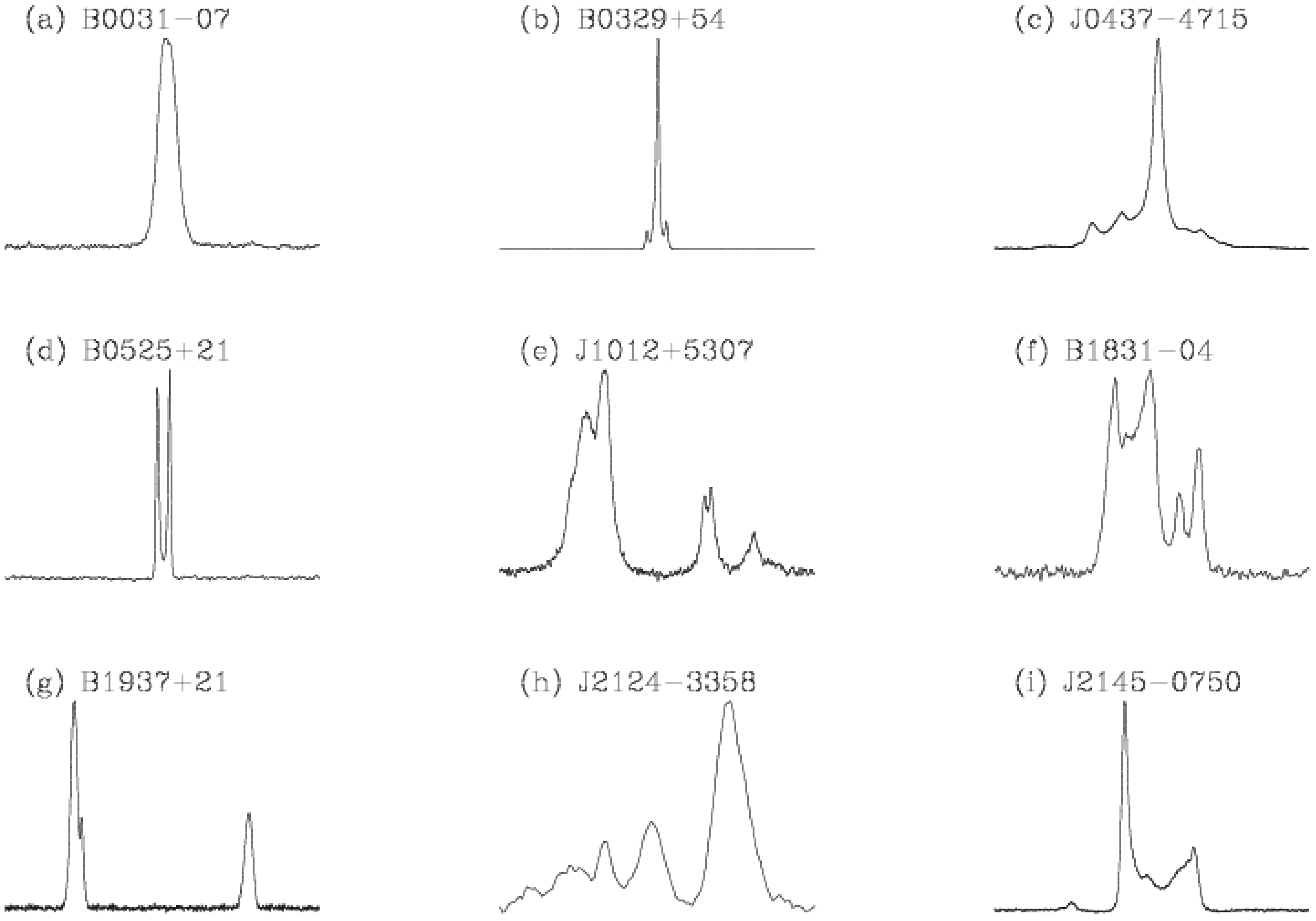

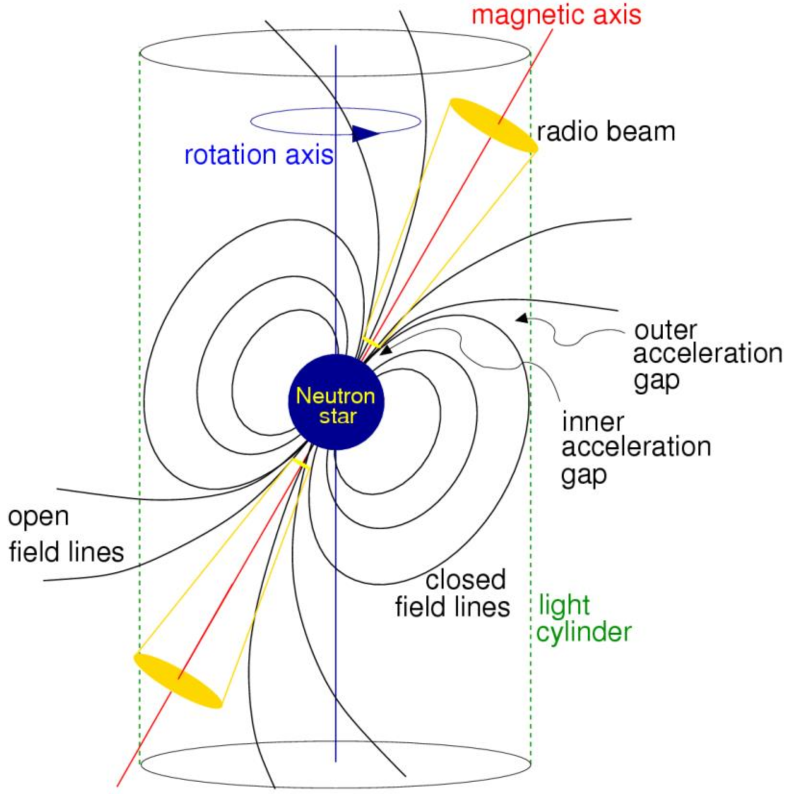

Chap 9 Zeeman

https://www.cv.nrao.edu/~sransom/web/Ch6.html

$$k = \frac{\omega}{v} = \frac{\omega}{c/n_r} \qquad n_r^2 = 1 - \frac{\omega_p^2}{\omega^2} \qquad \omega = \frac{k\,c}{n_r} = \frac{k\,c}{\sqrt{1 - \frac{\omega_p^2}{\omega^2}}}$$

$$\omega^2 - \omega_p^2 = k^2\,c^2 \qquad 2\omega\,d\omega = 2k\,dk\;c^2$$

$$\frac{d\omega}{dk} = \frac{k\,c}{\omega} = c\,n_r = c\sqrt{1 - \frac{\omega_p^2}{\omega^2}}$$

Pulses propagate at the group velocity, which is frequency dependent.

$$v_{\mathrm{group}} = \frac{d\omega}{dk} = c(1 - \frac{\omega_p^2}{\omega^2})^{1/2}$$

Pulse traveling time = $\tau = \int_0^L \frac{ds}{v_g} = \int \frac{ds}{c(1-\omega_p^2/\omega^2)^{1/2}}$

In ISM, $\omega^2 \gg \omega_p^2$, so $(1-\omega_p^2/\omega^2)^{-1/2} \approx (1+\omega_p^2/2\omega^2)$

$$\tau \approx \int_0^L \frac{ds}{c}(1+\omega_p^2/2\,\omega^2)$$

Since $\omega_p = \sqrt{4\pi\, n\, e^2/m}$, $\longrightarrow$ $\boxed{\tau \approx \frac{L}{c} + \frac{4\pi\, e^2}{2\, m\, \omega^2} \int_0^L n_e\, ds}$

Traveling time ←→ frequency

Signal arrives earlier at a higher frequency.

Dispersion Measure
(DM) [cm^{-3} pc];
typical DM = 10 – 200

For ω_1 and ω_2,

$$\Delta\tau = \frac{4\pi\, e^2}{2\, m}\left(\frac{1}{\omega_1^2} - \frac{1}{\omega_2^2}\right) = 4.1 \times 10^3\ DM\left(\frac{1}{\nu_1^2} - \frac{1}{\nu_2^2}\right)$$

in MHz

This gives DM → n_e along the line of sight

Observed $\langle n_e \rangle \sim 0.03$ to $0.08\ \mathrm{cm}^{-3}$

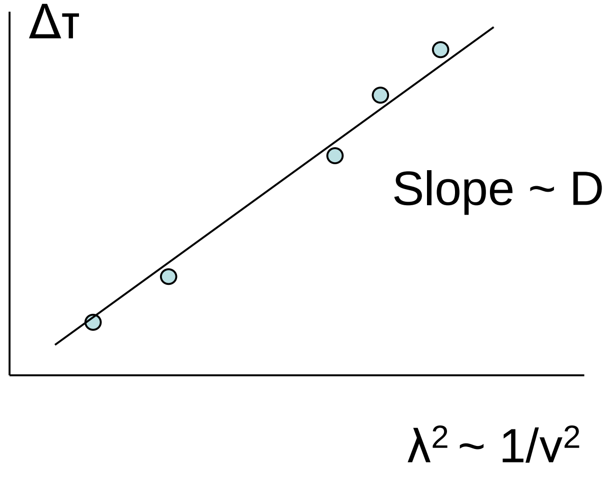

Alternatively, one can assume n_e and estimate the distance.

In fact, n_e varies along the line of sight → scintillation (terrestrial 1”, ISM 1 mas)

$\lvert b \rvert$	< 2	2-5	5-10	10-30	30-90
DM	142	60	59	37	13

Dispersion measure of the ISM from observations of 60 pulsars for various intervals of Galactic latitude b (from Scheffler & Elsässer 1987 based on Pottasch 1974)

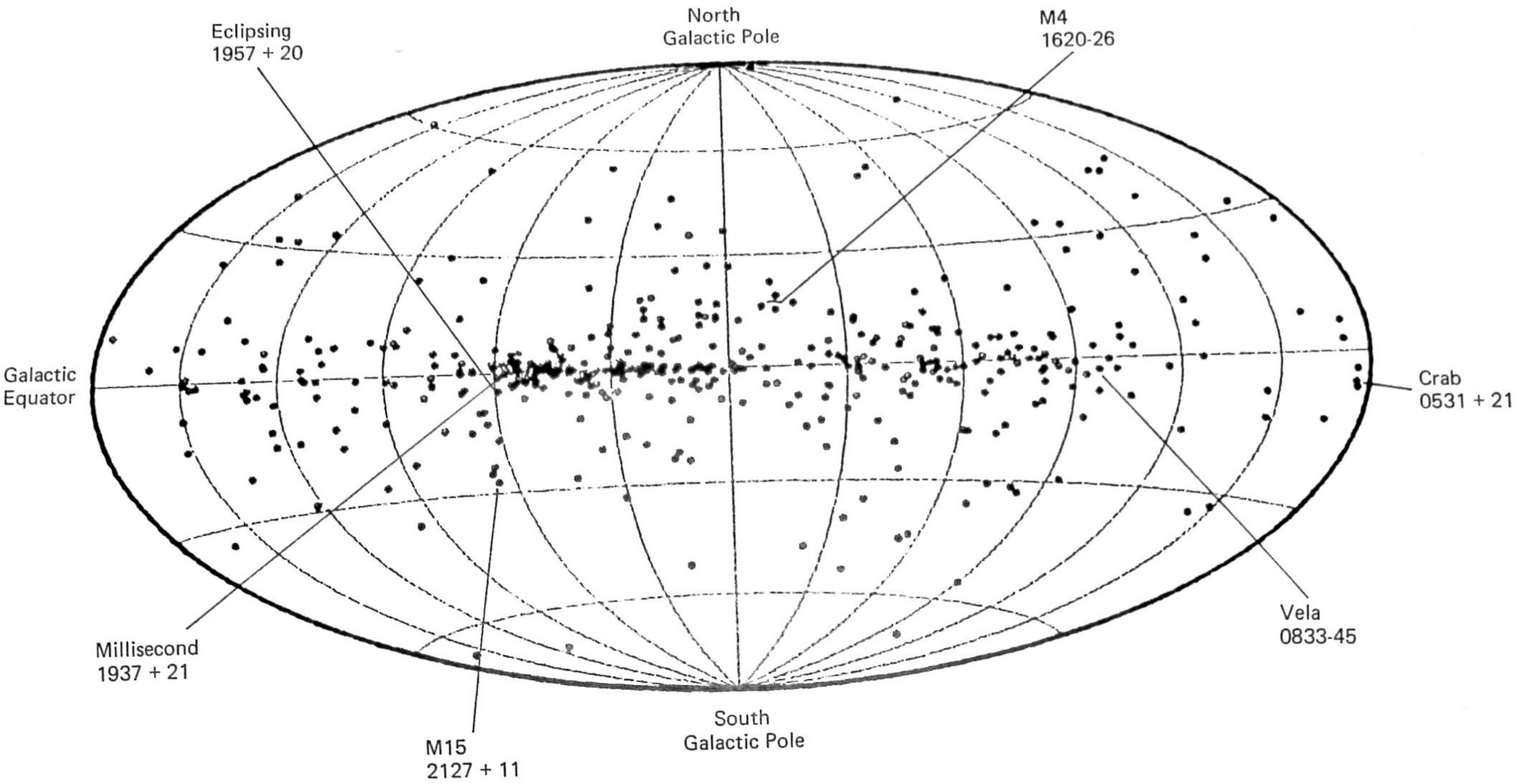

Pulsars in Galactic Coordinates

Faraday Rotation/Effect

What if there is magnetic field?

The effect in which the plane of polarization of an EM wave rotates under the influence of a magnetic field parallel to the direction of propagation

$$n_r^2 = 1 - \omega_p^2/\omega^2 \text{ is modified,} \longrightarrow \boxed{n_r^2 = 1 - \frac{\omega_p^2}{\omega(\omega \pm \omega_B})}$$

$$\text{where } \omega_B = \frac{e\,B}{m\,c} = \frac{4.8\times10^{-10}\times10^{-6}}{10^{-27}\times3\times10^{10}} \sim 10 \text{ [Hz]}$$

B → different n_r → different phase velocities (**circular birefringence**) for 2 opposite circular polarizations (linear polarization with a specific position angle) → PA rotates

In ISM, ω (~10^8 Hz) >> ω_p (~10^4 Hz) >> ω_B (~10 Hz)

Faraday Rotation --- rotation of the plane of polarization when light passes through a magnetic field

Circularly polarized light → $\boldsymbol{E}$ field rotates → force on the charged particles to make circular motion → creating its own $\boldsymbol{B}$ field, either parallel or in opposite direction to the external field → phase difference

➔ Change of position angle of the linear polarization

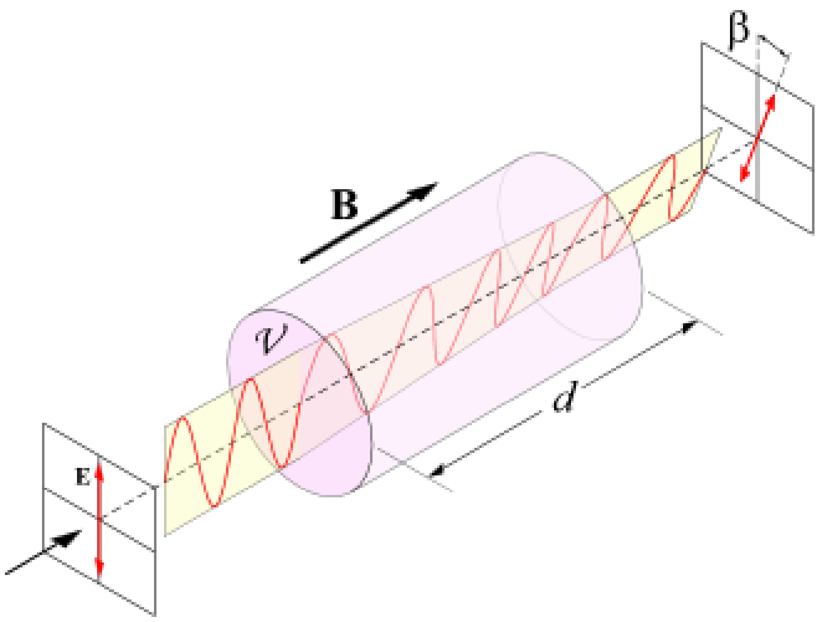

Faraday rotation angle $\beta = RM\,\lambda^2$ where the rotation measure (RM) is

$$\mathrm{RM} = \frac{e^3}{2\pi m^2 c^4}\int_0^d n_e(s) B_{\parallel}(s)\,\mathrm{ds}$$

$$\frac{\omega_p^2}{\omega^2(1 \pm \omega_B/\omega}) \approx \frac{\omega_p^2}{\omega^2}(1 \mp \omega_B/\omega)$$

original change

$$n_r^2 = 1 - \frac{\omega_p^2}{\omega^2} \pm \frac{\omega_p^2\,\omega_B}{\omega^3}$$

$$n_r = (1 - \frac{\omega_p^2}{\omega^2} \pm \frac{\omega_p^2\,\omega_B}{\omega^3})^{1/2} \approx (1 - \frac{\omega_p^2}{\omega^2} \pm \frac{\omega_p^2\,\omega_B}{2\omega^3}) \equiv n_{r,0} \pm \Delta n_r$$

$$\begin{aligned}
\text{Phase} \quad &= \quad \varphi = k\,n_r\,\mathfrak{z} = \frac{\omega}{c}\ \frac{\omega_p^2\,\omega_B}{2\omega^3}\mathfrak{z} \\
&= \quad \frac{\lambda^2}{8\pi^2 c^3}\ \frac{4\pi\,e^2}{m}\ \frac{e}{mc} \int B\,n\,ds \\
&\equiv \quad \lambda^2\ RM
\end{aligned}$$

Rotation Measure

$$\textbf{RM} = \frac{e^3}{2\pi m^2 c^4} \int n_e B_{\parallel} ds = 8.12 \times 10^5 \int_0^L n_e B_{\parallel} ds$$

ds [pc]; n_e [cm^{-3}]; B [Gauss]; λ [m]; φ[radian]

<u>Note</u>:

$$EM = \int n_e^2 \, ds$$

$$DM = \int n_e \, ds$$

$$RM = \int n_e B_{\parallel} \, ds$$

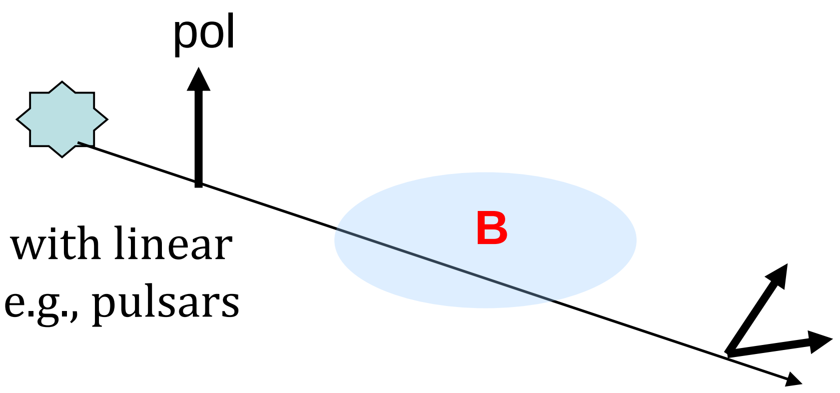

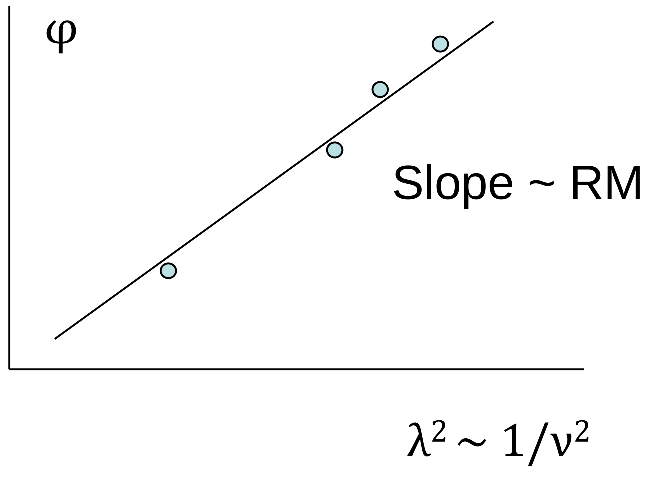

For polarized pulsars for which DMs are known

$$\frac{\int n_e B_{\|} ds}{\int n_e ds} = \frac{1}{8.1 \times 10^5} \frac{RM}{DM} = < B_{\|} >$$

e.g., B (Vela) $\sim 0.8\ \mu$G

For galaxies, guess n_e and get B

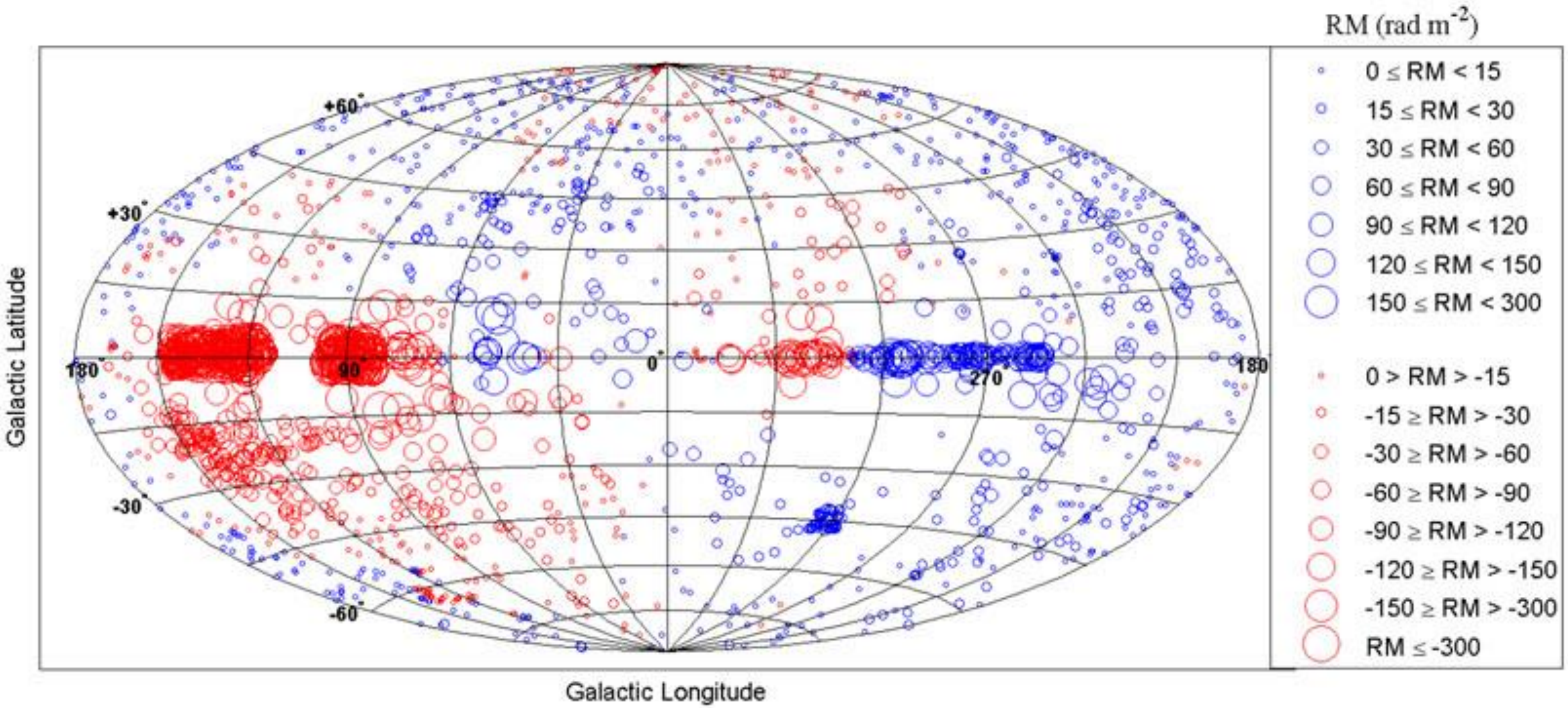

Figure 3. A smoothed representation of 2257 **Faraday rotation** measures in Galactic coordinates with the Galactic center at (0,0). (Kronberg & Newton-McGee, [3]). Blue and red circles represent positive and negative RM's respectively, and the circle size is proportional to RM strength.

http://ned.ipac.caltech.edu/level5/Sept10/Kronberg/Figures/figure3.jpg

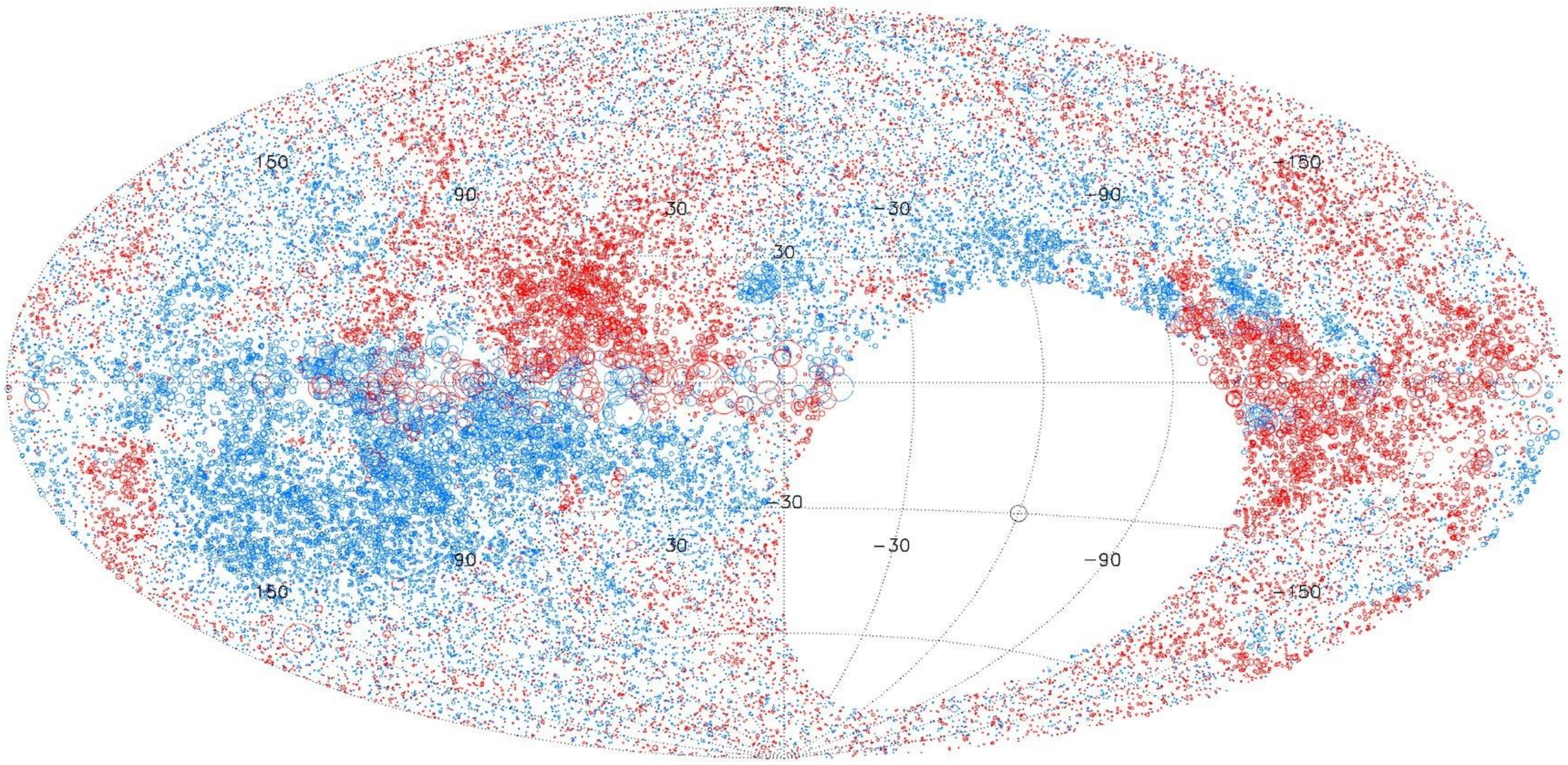

Plot of 37,543 RM values over the sky north of $\delta = -40°$.
Red circles are positive rotation measure and blue circles are negative. The size of each circle scales linearly with magnitude of rotation measure. (Taylor et al. 2009 ApJ, 702, 1230)

Note:

The Crab pulsar (PSR 0531+21) has been measured to have

$DM = 56.791\ \mathrm{cm}^{-3}\ \mathrm{pc}$, and $RM = -42.3\ \mathrm{m}^{-2}\ \mathrm{rad}$

→ mean longitudinal field of 0.92 micro-gauss (Manchester, Nat, 1971).

NATURE PHYSICAL SCIENCE VOL. 231 JUNE 28 1971

Rotation Measure and Intrinsic Angle of the Crab Pulsar Radio Emission

R. N. MANCHESTER
National Radio Astronomy Observatory, Green Bank, West Virginia 24944

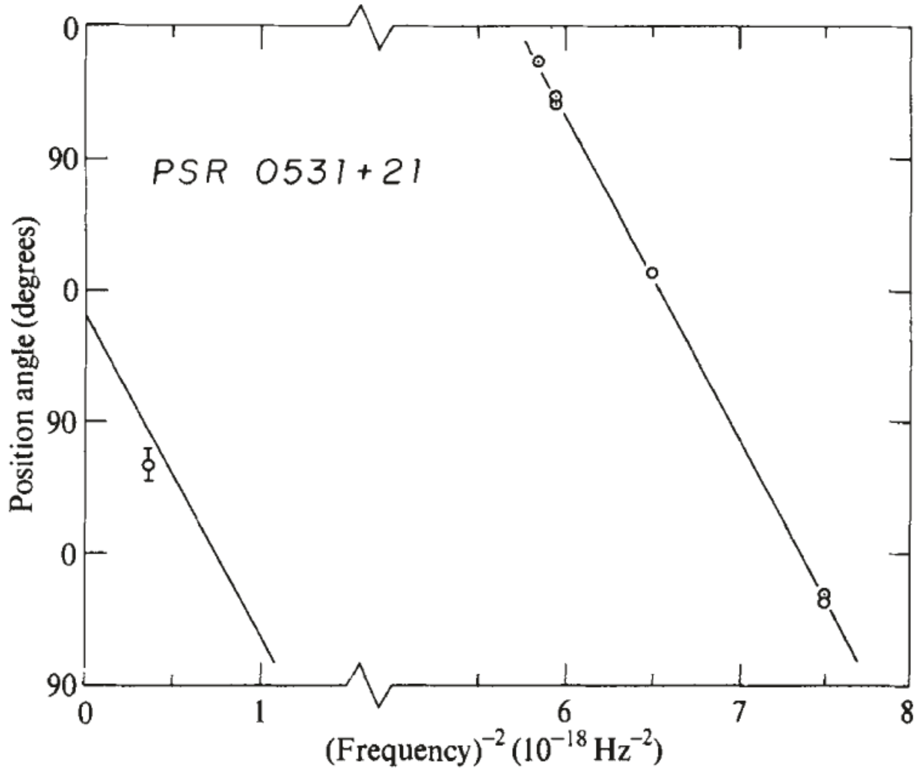

Milky Way (and galaxies)

- Primordial (seed) weak field (origin unknown) could not last $\xrightarrow{\text{dynamo}}$ a strong field

- Dynamo needs turbulence and differential rotation (alpha-Omega dynamo)
  - ✓ Spherical objects (stars/planets) → double torus near equator with a reversal
  - ✓ Flat objects (galactic disks) → single torus of spiral shape with no reversal

Rainer Beck (2007) Scholarpedia, 2, 2411

http://www.scholarpedia.org/article/Galactic_magnetic_fields#The_Origin_of_Galactic_Magnetic_Fields